International Journal of Nanomedicine

Dovepress
Taylor & Francis Group

Open Access Full Text Article

ORIGINAL RESEARCH

Lipid Nanoparticles Formulated with a Novel Cholesterol-Tailed Ionizable Lipid Markedly Increase mRNA Delivery Both in vitro and in vivo

Ju Hyeong Jeon[1], Huabin Zhu[1], Jane Qin[1], Luyao Wang[2], Stephanie Mou[1], Laura Katherine Langston[1], Ramesh Marasini[1], Jianzhu Chen[3], Renhuan Xu[1], Shuna Li[2], Xinle Cui[1]

[1]ARV Technologies, Inc, North Bethesda, MD, 20852, USA; [2]Department of Otorhinolaryngology-Head and Neck Surgery, Xinhua Hospital, Shanghai Jiaotong University School of Medicine, Shanghai, 200092, People's Republic of China; [3]Department of Biology and Koch Institute for Integrative Cancer Research, Massachusetts Institute of Technology, Cambridge, MA, 02139, USA

Correspondence: Shuna Li; Xinle Cui, Email lishuna@xinhuamed.com.cn; jcui@arv-tech.com

Background: Lipid nanoparticles (LNPs) have emerged as the most successful, effective, and safe method for RNA delivery, and have shown tremendous potential for the treatment of various diseases, such as messenger RNA (mRNA) vaccines, gene editing, and RNA interface (RNAi) therapies. The development of novel ionizable lipids holds great promise in improving the efficacy and safety of LNPs.

Methods: We synthesized a novel ionizable lipid, ARV-T1, with a cholesterol moiety incorporated in its tail. We characterized the physicochemical properties of LNPs formulated with ARV-T1, calculated the pKa of ARV-T1, and conducted in vitro and in vivo mRNA delivery studies.

Results: ARV-T1 has a pKa value of 6.73, and compared to SM-102, the ionizable lipid used in the Moderna SARS-CoV2 vaccine, the LNPs formulated with ARV-T1 showed smaller particle sizes, lower polydispersity indices, and higher absolute zeta potential values. More importantly, the LNPs formulated with ARV-T1 showed significantly increased mRNA delivery both in vitro and in vivo, markedly increased protein expression, and demonstrated more than 10-fold higher potency in inducing SARS-CoV-2 spike protein binding antibodies and SARS-CoV-2 virus neutralizing antibodies in mice compared to the LNPs formulated with SM-102. Furthermore, the unique ester linkage of ARV-T1 enables rapid and complete metabolism in vivo, thereby improving its biocompatibility and safety profile.

Conclusion: These findings suggest that the novel ionizable lipid ARV-T1 holds great promise for the development of mRNA vaccines and other mRNA-based therapeutics and may pave the way for the development of safer and more effective mRNA delivery systems.

Keywords: novel ionizable lipids, ribonucleic acid, protein expression, vaccine, neutralizing antibodies

Introduction

The rise of nucleic acid therapeutics, particularly messenger RNA (mRNA) based treatments delivered via lipid nanoparticles (LNPs), has been monumental and largely catalyzed by the global response to the COVID-19 pandemic.[1–3] mRNA and other RNA therapeutics have garnered significant attention owing to their ability to modulate gene expression in living organisms.[4,5] LNPs have been predominantly utilized for delivering RNA therapeutics, including small interfering RNA (siRNAs) and mRNA. Notably, clinically approved drugs such as Patisiran (Onpattro®) for siRNA, Tozinameran (Comirnaty®), and Elasomeran (Spikevax®) for mRNA have employed LNP-based delivery systems.[1,3,5]

Efficient in vivo delivery systems are pivotal for unlocking the full potential of RNA therapeutics. Ionizable lipid nanoparticles (LNPs) have emerged as a promising approach for this purpose.[6] Ionizable LNPs offer several advantages for RNA delivery. They shield nucleic acids from degradation by exogenous and endogenous nucleases, and facilitate

Received: 29 March 2025
Accepted: 15 July 2025
Published: 28 July 2025

cellular uptake and expression.[1,4] This is achieved through the pH-sensitive ionization of the amino lipid components and the surface properties of the LNPs. By controlling particle size and composition, ionizable LNPs can be tailored for organ- or tissue-specific delivery of mRNA, enhancing therapeutic efficacy while minimizing off-target effects.[6,7]

LNPs typically consist of ionizable lipids or lipid-like materials, helper lipids, cholesterol, and polyethylene glycol (PEG)-containing lipids.[1,6] Among these components, ionizable lipids play a pivotal role in the effectiveness of LNPs as delivery vehicles for RNA therapeutics and have emerged as a cornerstone of LNP research and development owing to their active role in nucleic acid delivery.[7,8] Ionizable lipids possess unique properties that make them highly suitable for this purpose. First, they are positively charged below their pKa, which facilitates the loading of negatively charged nucleic acid drugs during the self-assembly process into nanoparticles when LNPs are manufactured. This ensured the efficient encapsulation of the therapeutic cargo within the LNPs. Second, ionizable lipids become uncharged at physiological pH, minimizing potential off-target toxicity and increasing their half-life and circulation time in the body. Third, upon cellular uptake and exposure to the lower pH environment in the endosomes, ionizable lipids regain their positive charge, which could disrupt the endosome membrane and facilitate the escape of RNAs into the cytoplasm. This pH-dependent behavior of ionizable lipids is crucial for facilitating endosomal escape, allowing the release of nucleic acid payload into the cytoplasm, where it can exert its therapeutic effects.[3,7,9] Furthermore, ionizable lipids contribute to the physicochemical profile and stability of LNPs, influencing factors such as the particle size and surface properties.[7] These characteristics of ionizable lipids are critical for optimizing LNP formulations for specific therapeutic applications including vaccine development and cancer treatment.[1,3,8] Overall, the unique properties of ionizable lipids make them invaluable components of LNP systems, enabling targeted and efficient delivery of RNA therapeutics for a wide range of diseases.

The development of novel ionizable lipids holds great promise in enhancing the efficacy and safety of LNP-based mRNA formulations.[5,7,9] In this study, we identified a novel ionizable lipid from a group of candidates derived by the chemical modification of sterol-based compounds. This novel ionizable lipid, ARV-T1, has a cholesterol moiety incorporated in its tail, which could further facilitate RNA escape from endosomes owing to its greater physical hindrance. As a result, LNPs formulated with ARV-T1 showed increased mRNA delivery, increased level of protein expression, and induced 10-fold higher antibody titers against SARS-CoV-2 spike protein after immunization in mice compared to LNPs formulated with the conventional ionizable lipid SM-102, the ionizable lipid used in the Moderna SARS-CoV-2 mRNA vaccine.[1,7] Furthermore, ARV-T1 possesses a unique ester linkage that enables facile metabolism in vivo, similar to the lipids utilized in Tozinameran and Elasomeran, mRNA vaccines developed by Pfizer/BioNTech and Moderna.[4,8] This metabolic pathway enhances the biocompatibility of ARV-T1 and contributes to an improved safety profile.

Materials and Methods

Materials and Reagents

Cholesterol (plant-derived, catalog: 700100P) 1,2-distearoyl-sn-glycero-3-phosphocholine (DSPC, catalog: 850365) and 1,2-dimyristoyl-snglycero- 3-phosphoethanolamine-N-[methoxy(polyethylene glycol)-2000] (DMG-PEG2000, catalog: 880151P) were obtained from Avanti Polar Lipids, while SM-012 (catalog: BP-25499) was purchased from Broadpharm. Citrate Buffer (0.5 M, pH 4.0, SKU#: BB-2032) was purchased from Boston BioProducts. Amicon Ultra 4 Centrifugal Filter Unit, 30kDa (catalog: UFC803024) and Amicon Ultra 15 Centrifugal Filter Unit, 30kDa (catalog: UFC903024) were obtained from Millipore Sigma (Saint Louis, USA). Quant-it™ RiboGreen RNA Assay Kit (Catalog: R11491), Slide-A-Lyzer™ G2 Dialysis Cassettes, (10K MWCO, 3/5/15 mL), TE buffer pH 7.4 (catalog no: J60234.EQE), NuPAGE™ MES SDS Running Buffer (20X, catalog: NP0002), Pierce™ RIPA Buffer (catalog: 89900), Novex NuPAGE 4–12% Bis-Tris Mini Gels (catalog: NP0322BOX), NuPAGE™, Sample Reducing Agent (10X, catalog: 2398613), NuPAGE™ LDS Sample Buffer (4X, catalog: 2466926), Pierce™ ECL Western Blotting Substrate (catalog: 32209), Pierce™ BCA Protein Assay Kit (catalog: 23225), Iblot™ 2 Transfer Stacks, PVDF (mini catalog: IB24002), and Lipofectamine™ MessengerMAX™ Transfection Reagent (catalog: LMRNA008) were purchased from the Thermo Fisher Scientific, USA. 6-(p-Toluidino)-2-naphthalenesulfonic acid sodium salt (catalog: T9792), Formaldehyde (catalog:

252549), Triton™ X-100 (catalog: X100), and Tween 20 (catalog: P7949) were purchased from Sigma Aldrich, Saint Louis, USA.

Synthesis of the Proprietary Ionizable Lipid ARV-T1 and Other Related Lipids

The ionizable lipid ARV-T1 was synthesized using 1-bromooctane, heptanal, 7-bromoheptanoic acid, 4-aminobutan-1-ol, and cholesterol in a series of six chemical reaction steps (Figure 1). Briefly, Step 1: Incubated 1-bromooctane with Mg and I_2 in tetrahydrofuran (THF) at 30 to 40°C for 1 h to produce Compound 2. Step 2: Cooled Compound 2 to 0°C, added heptanal and incubated at 25°C for 16 h, extracted the reaction with ethyl acetate, dried with anhydrous Na_2SO_4 and purified by column chromatography to obtain Compound 3. Step 3: Added Compound 3 and 7-bromoheptanoic acid in dichloromethane, incubated with EDCI, DIEA, and DMAP for 16 h at 25°C to produce Compound 4 and purified. Step 4: Added Compound 4 and 4-aminobutan-1-ol in ethanol and incubated at 65°C for 16 h, extracted the reaction with ethyl acetate, washed with saturated brine, dried with anhydrous Na_2SO_4 and purified by column chromatography to obtain Compound 5. Added cholesterol and 6-bromohexanoic acid in dichloromethane, incubated with EDCI, DIEA, and DMAP for 16 h at 25°C to produce Compound 5a and purified. Step 6: Added Compounds 5 and 5a in acetonitrile (ACN), incubated with K_2CO_3, KI, and CPME at 90°C for 16 h, dissolved in dichloromethane, filtered, and purified by column chromatography to produce ionizable lipid ARV-T1. Additional ionizable lipids ARV-T2, T3 and T4 were synthesized using a similar approach.

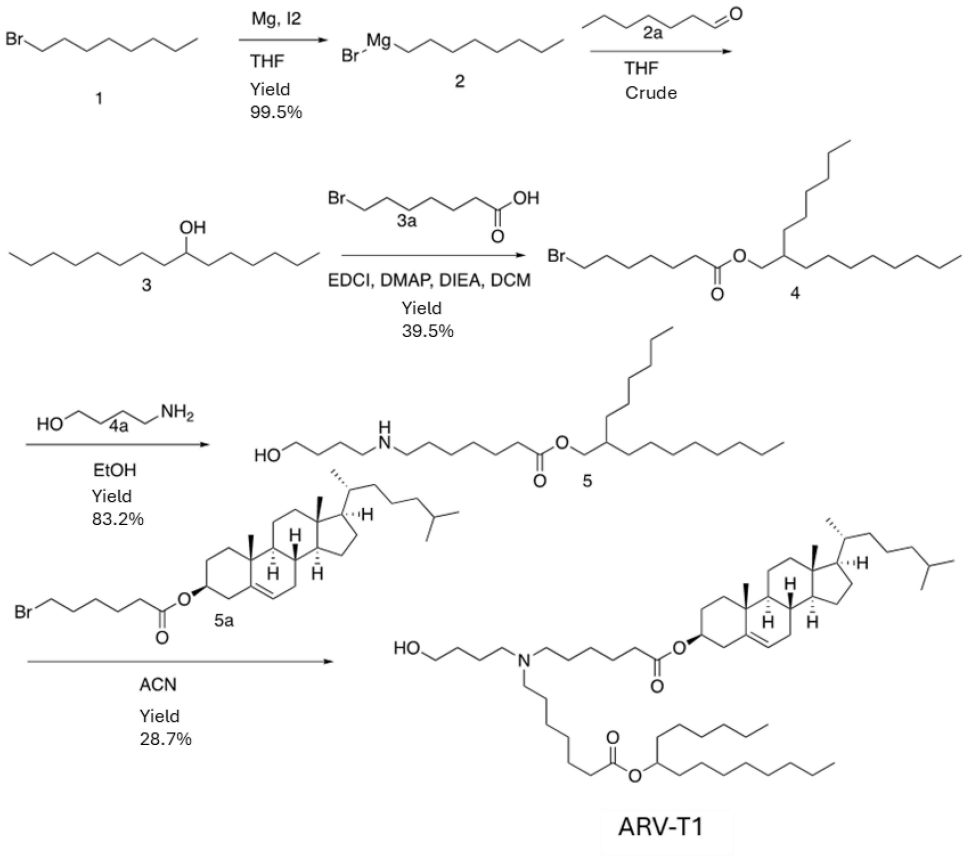

Figure 1 Synthesis of the novel ionizable lipid ARV-T1. Raw materials 1-bromooctane, heptanal, 7-bromoheptanoic acid, 6-bromohexanoic acid and cholesterol were used to synthesize ARV-T1 through a series of 6 steps of chemical reactions. Final product of ARV-T1 was purified as white power.

https://doi.org/10.2147/IJN.S527822

Animal Studies

BALB/c mice were bred and maintained at an animal facility in Noble Life Sciences (NLS Woodbine, MD, USA). LNP Biodistribution, toxicology, and immunization studies were conducted using 6 to 8-week-old female mice, and all procedures were conducted at Noble Life Science Inc. following the standard IACUC protocol (NLS21-A59-102). All the mouse studies were reviewed and approved by the Animal Ethics Committee of Noble Life Science Inc. and the Institutional Review Board of ARV. All animal care and treatments followed the guidelines of Guide for the Care and Use of Laboratory Animals (8th Edition, National Research Council).

In vitro mRNA Transcription and LNP Formulation

Sequence-optimized mRNA encoding the spike protein of the SARS-CoV-2 delta variant was synthesized and cloned into the pUC57 vector with the 5′ untranslated region (UTR) and 3′ UTR. In vitro transcription was performed using an optimized T7 RNA polymerase-mediated transcription reaction with uridine-5′-triphosphate replaced by N1-methylpseudouridine-5′-triphosphate.[10] The in vitro transcription DNA template contained the target open reading frame flanked by the 5′ and 3′ UTRs, and an encoded polyA tail. After transcription, a cap 1 structure was enzymatically added using a vaccinia capping enzyme and 2′O-methyltransferase (New England Biolabs, MA, USA). The synthesized mRNA was purified by LiCl precipitation and sterilized by filtration.

LNP formulations were prepared by mixing lipids in an organic phase (ethanol) with mRNA in an aqueous phase (50 mM citrate buffer, pH 4.0). A NanoAssemblr® Ignite system (Precision Nanosystem, Vancouver, Canada) was used for formulation, maintaining a specific ratio (1:3, v/v) between the organic and aqueous phases. The total lipid concentration was 12.5 mM, with the molar percentage ratio for constituent lipids as: 50% ATV-T1 (ionizable lipids), 10% DSPC, 38.5% cholesterol, and 1.5% DMG-PEG in ethanol. All formulations maintained a nitrogen-to-phosphate ratio (N/P) of 4. The formulated product was dialyzed against 10 mM Tris-HCl (pH 7.4) with 8% sucrose for 16 h to remove any residual ethanol and other impurities. The particles were concentrated using an Amicon ultra centrifugal filter (MWCO 30kDa) and passed through a 0.22μm syringe filter. LNPs were stored at −80°C in 10 mM Tris-HCL (pH 7.4) with 8% sucrose until use. LNPs formulated with the ionizable lipid SM-102, the ionizable lipid used in the Moderna SARS-CoV2 vaccine, were used as controls throughout the studies.

In situ Determination of pKa Using TNS Reagent

A series of buffers with pH ranging between 2.5 and 11.6 were prepared by adjusting the pH with 1 M HCl (or 1 M NaOH) of a solution containing 10 mM citrate, 10 mM phosphate, 10 mM borate, and 150 mM NaCl. Ninety microliters (90 μL) of each pH unit of buffer was added to a 96-well plate in triplicate, and 10 μL of empty LNP vehicle (prepared without mRNA) was added to each well (total 100 μL) to obtain an ionizable lipid concentration of 22 μM at each pH unit. A 300-μM stock solution of 6-(p-toluidino)-2-naphthalenesulfonic acid sodium (TNS reagent) was prepared in DMSO, and a calculated amount of this solution was added to each well of the buffer solutions containing LNPs to obtain a final concentration of 6 μM. After mixing by pipetting, the fluorescence of the resulting solution was read on a Perkin Elmer Microplate reader using an excitation wavelength of 325 nm and an emission wavelength of 435 nm. A sigmoidal plot of the fluorescence signal against pH was obtained using the GraphPad Prism Software. The pH at which half of the maximum fluorescence was reached was reported as the apparent pKa of the LNP.

Calculation of the mRNA Encapsulation Efficiency of LNP

After LNP formulation, the total encapsulated and unbound mRNA concentrations were determined using the Quant-iT RiboGreen RNA assay kit in the presence or absence of 0.5% (vol/vol) Triton-X-100 following the manufacturer's recommendations (Thermo Fischer Scientific). Briefly, RNA standard curve was prepared using 1% Triton-X-100 in TE buffer at concentrations from 0–1 μg/mL. In a 96-well plate, 50 μL of the LNP formulation was added to each well, followed by adding 50 μL of 1x TE buffer to measure free/unbound RNA or 50 μL of 2% Triton-X-100 in TE buffer to measure encapsulated RNA. Calcium and magnesium-free 1x phosphate buffered saline (DPBS) was used as blank. The plate was incubated at 37°C for 10 min, followed by adding 100 μL of 1:200 ratio of RiboGreen dye solution in 1x TE to

each well. Fluorescence was measured using a Perkin Elmer Microplate reader at an excitation wavelength of 485 nm and an emission wavelength of 530 nm. All experiments were conducted in duplicates. mRNA encapsulation efficiency (EE) was calculated using the following formula:

$$EE\ (\%) = 100 \times (\text{mRNA total} - \text{mRNA unbound})/\text{mRNA total}$$

Characterization of the Physicochemical Properties of LNP and Morphology of LNP

The average particle size and polydispersity index (PDI) of the LNPs were measured by dynamic light scattering (He–Ne laser, $\lambda = 632$ nm; detection angle = 173°) at 25°C using a ZetaSizer-Ultra Red (Malvern Panalytical, UK) in disposable low-volume (40 μL) clear polystyrene cuvettes (catalog: ZEN0040). Zeta potential was measured in disposable folded capillary cells (catalog: DTS1070) after diluting the LNPs to 800 μL with 1 × PBS. All experiments were conducted in triplicates. The morphology of the LNP was characterized by transmission electron microscopy (TEM).

Determination of LNP Stability

The stability of LNPs in serum was determined by agarose gel electrophoresis. Three hundred microliters of 1 mg/mL LNPs encapsulating SARS-CoV-2 delta variant spike protein mRNA were mixed with 300 μL of fetal bovine serum (FBS) and incubated at 37°C for 24 h, and 300 μL of 1 mg/mL SARSCoV-2 delta variant spike protein mRNA mixed with 300 μL FBS was incubated for 10 min at 37°C. The mRNA from the serum mixture or from the LNPs with/without serum treatment was isolated using TRIzol reagent, and the isolated mRNA concentration was determined using Nanodrop Lite. 3-(N-morpholino) propanesulfonic acid (MOPS)-denaturing gel (0.8% agarose gel) was prepared using agar, 10X MOPS buffer, formaldehyde solution, and nuclease-free water, and GelRed Nucleic Acid Gel Stain was added for gel staining. The mRNA isolated from mRNA + serum, LNP + serum, mRNA only or LNP only were incubated at 65°C for 5 min. RNA samples were then loaded onto the gel and run in 1X MOPS at 100 V for 45 min, and the RNA bands were analyzed. The stability under physiological conditions was also characterized by dispersing nanoparticles in PBS (pH 7.4) with 8% sucrose at a particle concentration of 1 mg/mL, stored at 4°C, −20°C, and −80°C for 24 weeks, followed by measuring the particle size, PDI, zeta potential using dynamic light scattering (He–Ne laser, $\lambda = 632$ nm; detection angle = 173°) and calculated mRNA encapsulation efficiency using RiboGreen Assay. Stability parameters were measured at weeks 0, 1, 2, 4, 8, 12, 16, and 24.

In vitro mRNA/Plasmid DNA Delivery and Cytotoxicity Analysis

To assess the in vitro delivery efficiency, HEK-293T cells were transfected with LNP-mRNA encoding the SARS-CoV-2 delta variant spike protein, formulated with ARV-T1 in comparison to SM-102, and the expression of spike proteins was evaluated by Western blotting and flow cytometry analysis. For Western blotting, 25 μg of protein from the cell lysis of 293T cells transfected with LNP-mRNA was separated by SDS-PAGE and transferred to a PVDF membrane. The PVDF membrane was then incubated with the primary spike S2 antibody (ThermoFisher Scientific), followed by incubation with horseradish peroxidase (HRP)-conjugated anti-mouse immunoglobulin G (IgG) secondary antibody (Cell Signaling Technology). The membrane was developed using Signal Fire ECL chemiluminescence reagent, and the images were captured using a Bio-imager (Perkin Elmer). For flow cytometry analysis, HEK-293T cells were seeded at 4.8×10^5 cells per well in a 6-well plate and cultured for 24 h, followed by transfection with LNPs encapsulating SARS-CoV-2 delta variant spike protein mRNA. Cells were trypsinized, washed with cold PBS twice, and resuspended in 500 μL of cold 5% FBS in PBS for flow cytometry analysis.

To determine whether the LNPs formulated with ARV-T1 could also deliver plasmid DNA effectively, the eGFP gene was cloned into the pcDNA3.1 vector and was driven by the CMV promoter (Thermo Fisher Scientific), and LNPs encapsulating pcDNA3.1-eGFP were produced in the same way as that of LNPs encapsulating mRNA, as described in section 2.4. Transfection of HEK 293T cells with LNPs formulated with ARV-T1 encapsulating pcDNA3.1-eGFP was performed as described above, and eGFP expression was analyzed by fluorescence microscopy.

Cell viability was analyzed using the XTT assay. Briefly, HEK 293T cells were seeded at a density of 1.5×10^4 cells/well in a 96-well plate and cultured overnight. The cells were then incubated with different concentrations of LNPs

encapsulating SARS-CoV-2 delta variant spike protein mRNA for 24 h. After washing twice with PBS, the cells were incubated with 100 μL of 5 mg/mL XTT in PBS for 4 h, the supernatant was carefully aspirated, and intracellular formazan crystals were dissolved in DMSO. The absorbance of the formazan solution was measured at 570 nm wavelength using a spectrophotometer.

Cell viability (%) was expressed as a percentage relative to that of untreated cells.

Characterization of LNP Biodistribution

LNP formulated with ARV-T1 encapsulating mRNA encoding firefly luciferase was measured by whole-body imaging post-IM injection in BALB/c mice using an IVIS imaging system. LNP formulated with SM-102 encapsulating mRNA encoding firefly luciferase was used as a control. Time-dependent organ luminescence was quantified after injection into the flanks of BALB/c mice (n = 6) at a dose of 1μg Luc mRNA encapsulated in the LNP. The mice were anesthetized *using 3–5% Isoflurane* and imaged at 6, 24, 48, and 72 h post-injection. All procedures were conducted at Noble Life Science Inc. following the standard IACUC protocol (NLS21-A59-102).

Mouse Immunization and Binding Antibody Analysis

For immunogenicity studies, BALB/c mice were immunized intramuscularly (quadriceps) with LNPs encapsulating SARS-CoV-2 delta variant spike protein mRNA formulated with ARV-T1 in comparison to SM-102 on day 1 (prime) and day 21 (boost), and PBS was injected as a negative control.

Serum was collected two weeks after priming and boosting. The murine antibody response to the SARS-CoV-2 spike protein was assessed using an indirect enzyme-linked immunosorbent assay (ELISA).

ELISA plates (Nunc MaxiSorp, Thermofisher, Cat#44-2404-21) were coated with 1μg/mL recombinant SARS-CoV-2 spike protein (Sino Biological Inc., Cat#40591-V08H) overnight and blocked with 2% BSA in PBS. Mouse sera collected on days 14 and 35 post-primary immunization were used for ELISA analysis.

Serum samples were diluted 1 to 100, followed by 1:5 serial dilution for 8 times with 0.2% BSA in PBS. The samples were added to the wells of a 96-well plate in duplicates and incubated for 1 h at room temperature. After washing 3 times with 0.05% Tween 20 in PBS, 1:2000 goat anti-mouse IgG-HRP (Southern Biotech, Cat# 1031–05) was added and incubated for 1 h at room temperature. The reaction was developed using TMB Substrate (Sigma, Cat#T0440-1001) and stopped with TMB Stop Solution (Invitrogen, Cat#SS04). The plates were read at 450 nm wavelength using an Epoch ELISA reader (BioTek, Winooski, VT, USA). Convalescent serum derived from COVID-positive human serum (RayBiotech) was used as the positive control.

SARS-CoV-2 Neutralization Analysis

SARS-CoV-2 pseudo-viruses expressing a luciferase reporter gene were purchased from Codex BioSolutions. To determine the neutralization activity of the antisera from vaccinated mice, HEK293T-hACE2 cells were seeded in 384-well tissue culture plates at a density of 7.5×10^3 cells per well and cultured overnight. Two-fold serial dilutions of heat-inactivated serum samples were prepared and each 17.5 μL was mixed with 7.5 μL of pseudovirus and incubated at 37°C for 1 h. The serum pseudovirus mixture was added to HEK293T-hACE2 cells and cultured for 48 h. The cells were then lysed, and the Steady-Glo Luciferase Assay (Promega) was performed according to the manufacturer's instructions.

SARS-CoV-2 neutralization titers were defined as the sample dilution at which a 50% reduction in relative light units (IC50) relative to the average of the virus control wells. Convalescent serum derived from COVID-positive human serum (RayBiotech) was used as the positive control.

In vivo Toxicity Study of LNPs

BALB/c mice (five in each group) were immunized with 5 or 10 μg LNPs encapsulating SARS-CoV-2 spike protein mRNA formulated with ARV-T1 versus SM 102, and PBS was used as the negative control. The mice were immunized twice at 3-week intervals, and blood was drawn 1 d after the last immunization for biochemical testing, and immunohistochemical analysis of the liver, heart, and kidney was performed 2 weeks after the last immunization.

Statistics

T-test, one-way ANOVA, and dose-response inhibition model fit were conducted using GraphPad Prism software. All data are presented as mean ± standard deviation. Statistical significance was set at $p < 0.05$.

Results

LNPs Formulated with ARV-T1 Had Smaller Particle Size, Lower Polydispersity Index and Higher Absolute Zeta Potential Value Compared to the LNPs Formulated with SM-102

An amino lipid head group containing the novel ionizable lipid ARV-T1 was identified through initial screening of a broad range of synthesized chemical compounds (Figure 1). This lipid was found to efficiently drive mRNA encapsulation, indicating its potential for use in LNP formulations (Figure 2B). Upon chemical modification of the butanolamine head group with cholesterol and an alkoxy alkanoate moiety, the novel ionizable lipid ARV-T1 formulated

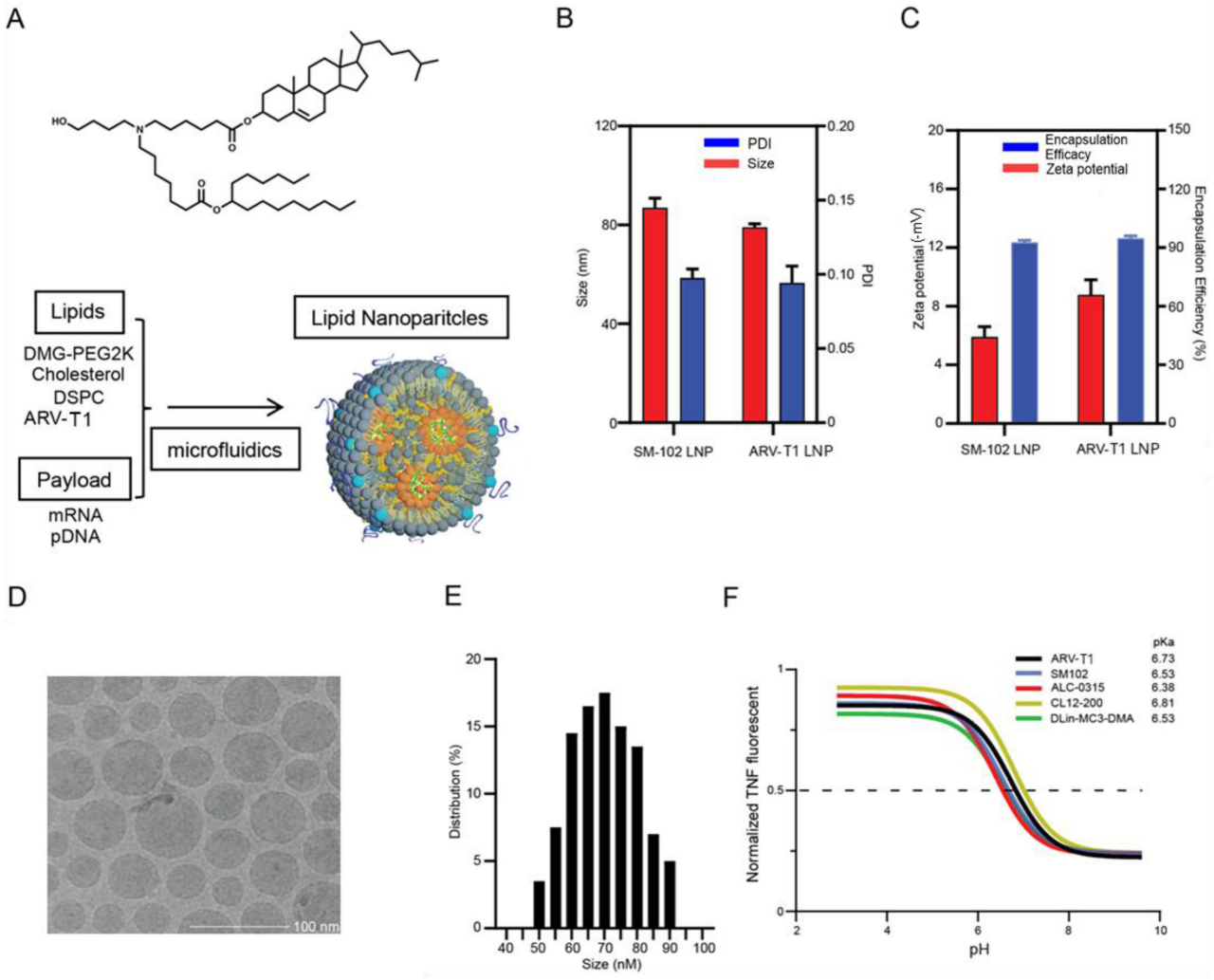

Figure 2 Characterization of LNPs formulated with the novel ionizable lipid ARV-T1. (**A**) Diagram of the structure of ARV-T1 and the production of LNPs. (**B**) Size and PDI of the LNPs formulated with ARV-T1 as comparison to that of SM-102. (**C**) Zeta potential and encapsulation efficacy of the LNPs formulated with ARV-T1 and SM-102. (**D**) Cryo-TEM image of LNPs formulated with ARV-T1. (**E**) Size distribution of the LNPs formulated with ARV-T1. (**F**) The pKa value the LNPs formulated with ARV-T1 in comparison to that of the LNPs formulated with known ionizable lipids, the means of triplicates were used to conduct nonlinear regression curve fitting analysis. Compared to the ionizable lipid used in the Moderna SARS-CoV2 vaccine SM-102, the LNPs formulated with ARV-T1 demonstrated smaller particle size, lower polydispersity index and higher absolute zeta potential value and slightly higher encapsulation efficacy.

https://doi.org/10.2147/IJN.S527822

LNPs demonstrated small particle size and low polydispersity index (PDI) (Figure 2B). The ionizable lipid ARV-T1 contains a tertiary amine with ester-containing lipid tails, and these structural features enable rapid in vivo metabolism, thereby potentially improving the biocompatibility and clearance of LNPs (Figures 1 and 2A).[11,12] The physicochemical properties of the LNPs formulated with ARV-T1 demonstrated favorable characteristics for mRNA delivery, including efficient encapsulation, small size, and low polydispersity, suggesting that this novel ionizable lipid may hold great promise for use in mRNA-based therapeutics, especially vaccines.[12]

To characterize the ionizable properties of LNPs formulated using the novel ionizable lipid ARV-T1, we evaluated the apparent pKa of LNPs without mRNA encapsulated. The pKa of each LNP was determined using a 2-(p-toluidine)-6-naphthalene sulfonic acid (TNS) assay.[12,13] The formulated LNPs were incubated in a series of buffers with pH values ranging from 2.5 to 11.0, and the fluorescence intensity was analyzed. A sigmoidal curve fit analysis was performed plotting fluorescence intensity against pH (Figure 2F), and the pKa of LNPs was calculated (pH at 50% of maximum fluorescence). Because anionic TNS interacts with positively charged ionizable lipids and becomes lipophilic, when the pH value approaches the pKa value of LNP, less positively charged ionizable lipids are available to bind to TNS, and TNS becomes less lipophilic (more hydrophilic); therefore, more water molecules can quench the TNS fluorescence. Among the ARV-tech ionizable lipid libraries, ARV-T1 produced a sharp sigmoidal shaped curve with a pKa value of 6.73, which was close to the pKa values of the commercially available ionizable lipids SM-102, ALC-0315, C12-200, and DLin-MC3-DMA (6.53, 6.38, 6.81, and 6.53, respectively) (Figure 2F). The structural modification introduced into ARV-T1 was sufficient to affect the pKa value without changing the molecular dimensions of the hydrophilic region. It has been shown that amino lipids with a small head group allow preferential adoption of inverted hexagonal non-bilayer structures, which are believed to be the key factor for endosomal membrane fusion-mediated delivery of mRNA cargo to the cytosol of target cells by escaping endosomal degradation upon acidification.[14,15] More importantly, the cholesterol moiety incorporated in the tail of ARV-T1 could significantly facilitate mRNA escape owing to its unsymmetry and greater physical hindrance (Figures 1 and 2A).

We also characterized the diameter, polydispersity index (PDI), zeta potential, and encapsulation efficiency of the mRNA of the LNPs formulated using the microfluidic device (Figure 2A–C). LNPs formulated with ARV-T1 had about 80 nm mean hydrodynamic size and 0.09 PDI, while control LNPs formulated with SM-102 had about 90 nm and 0.10 for size and PDI, respectively (Figure 2B). The zeta potential values of the LNPs formulated with ARV-T1 and SM-102 were −10 mV and −5 mV, respectively, as analyzed using molecular biology grade water (Quality Biologicals) (Figure 2C). Since a higher charge of ionizable lipid is associated with more efficient encapsulation of nucleic acids in formulated LNPs, the higher absolute zeta potential value of the LNPs formulated with ARV-T1 could indicate higher nucleic acid encapsulation.[8,16] Although the encapsulation efficacy of the LNPs formulated with ARV-T1 was slightly higher than that of SM-102, all the formulated LNPs had RNA encapsulation efficacy above 90% (Figure 1C). Finally, the physical morphology of the LNPs was determined using cryo-transmission electron microscopy (cryo-TEM), which showed highly monodispersed and spherical particles with a size distribution ranging from 50 to 90 nm (Figure 1D and E). The difference in size between cryo-TEM and hydrodynamic size indicated that lipid-PEG provided a hydrating layer over the surface of the LNPs. Thus, the formed hydrating layers could enhance nanoparticle stability, help minimize protein corona formation in the bloodstream, and prevent LNPs from immune invasion.[17]

LNPs Formulated with ARV-T1 Demonstrated Significantly Higher-Level Delivery of mRNA and Higher-Level Protein Expression in vitro

To evaluate the ability of LNPs formulated with the ionizable lipid ARV-T1 to deliver mRNA in vitro, transfection of HEK 293T cells with LNPs encapsulating eGFP mRNA was conducted. Upon transfection of HEK 293T cells with 2.5 μg eGFP-mRNA per well in a 6-well plate, LNPs formulated with ARV-T1 were more efficient *in* mRNA delivery in vitro than LNPs formulated with SM-102, the ionizable lipid used in the Spikevax vaccine against SARS-CoV-2 (Figure 2A–C). The median signal intensity obtained from the LNP formulated with ARV-T1 transfected cell was approximately 7-fold higher than that of the LNP formulated with SM-102 transfected cell as shown in Figure 3C, although the LNPs formulated with ARV-T1 and SM-102 both showed more than 97% cells were GFP positive after transfection.

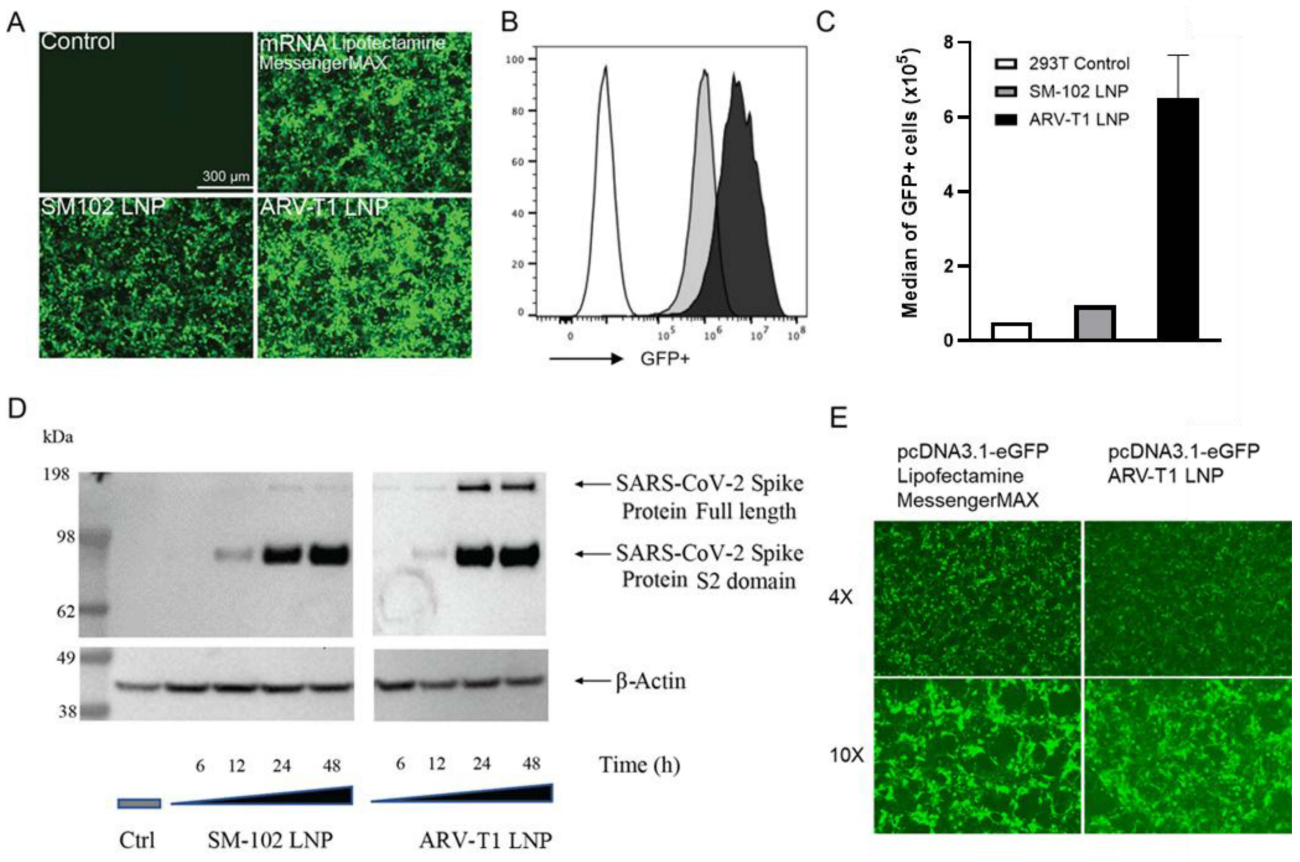

Figure 3 In vitro delivery of mRNA and protein expression by LNPs formulated with ARV-T1 were significantly higher than that of SM-102. LNPs formulated with ARV-T1 also delivered plasmid DNA effectively in vitro. (**A**–**C**). HEK293 cells were transfected with LNPs encapsulating eGFP mRNA formulated with either ARV-T1 or SM-102, the HEK293 cells transfected with LNPs formulated with ARV-T1 showed significantly higher GFP expression with fluorescent microscopy and flow cytometry analysis. (**D**) HEK293 cells transfected with LNPs encapsulating SARS-CoV-2 spike protein mRNA formulated with ARV-T1 demonstrated higher spike protein expression by Western blot analysis in comparison to the LNPs formulated with SM-102, especially the expression of full-length spike protein. (**E**) HEK 293 cells transfected with LNP formulated with ARV-T1 encapsulating pcDNA3.1-eGFP showed similar GFP expression compared to the HEK293 cells transfected with pcDNA3.1-eGFP-lipofectamin MassengerMax complex.

In addition, HEK293T cells were transfected with LNPs encapsulating SARS-CoV-2 delta variant spike protein mRNA formulated with ARV-T1 in comparison to SM-102, and the expression of SARS-CoV-2 spike protein was compared via Western blotting and flow cytometry analysis using a specific anti-SARS-CoV-2 S2 antibody. As shown in Figure 3D, the SARS-CoV-2 spike protein showed increased expression as the incubation time increased and reached a peak level of expression after 24 h. Furthermore, SARS-CoV-2 spike protein expression in 293T cells transfected with LNPs formulated with ARV-T1 was significantly higher than that of the 293T cells transfected with LNPs formulated with SM-102 (Figure 3D). This result led us to hypothesize that LNPs formulated with ARV-T1 could be more immunogenic in vivo and, therefore, could be a better vaccine candidate for SARS-CoV-2.

LNPs formulated with ARV-T1 showed promising results not only for mRNA delivery but also for plasmid DNA (pDNA) delivery. As shown in Figure 3E, transfection of HEK 293 cells with LNP formulated with ARV-T1 encapsulating pcDNA3.1-eGFP showed GFP expression similar to that of HEK293 cells transfected with pcDNA3.1-eGFP-lipofectamin MassengerMax complex.

LNPs Formulated with ARV-T1 Stored at −20°C for 12 weeks Showed No Significant Difference in Particle Size, PDI, Zeta Potential, Encapsulation Efficacy, and Demonstrated Similar Level of Protein Expression as Compared to the LNPs Stored at −80°C

One of the key functions of LNP is the protection of the encapsulated mRNA from degradation by the enzymes in the blood and tissue. As shown in Figure 4A, incubation of SARS-CoV-2 spike protein mRNA with FBS for 10 min resulted

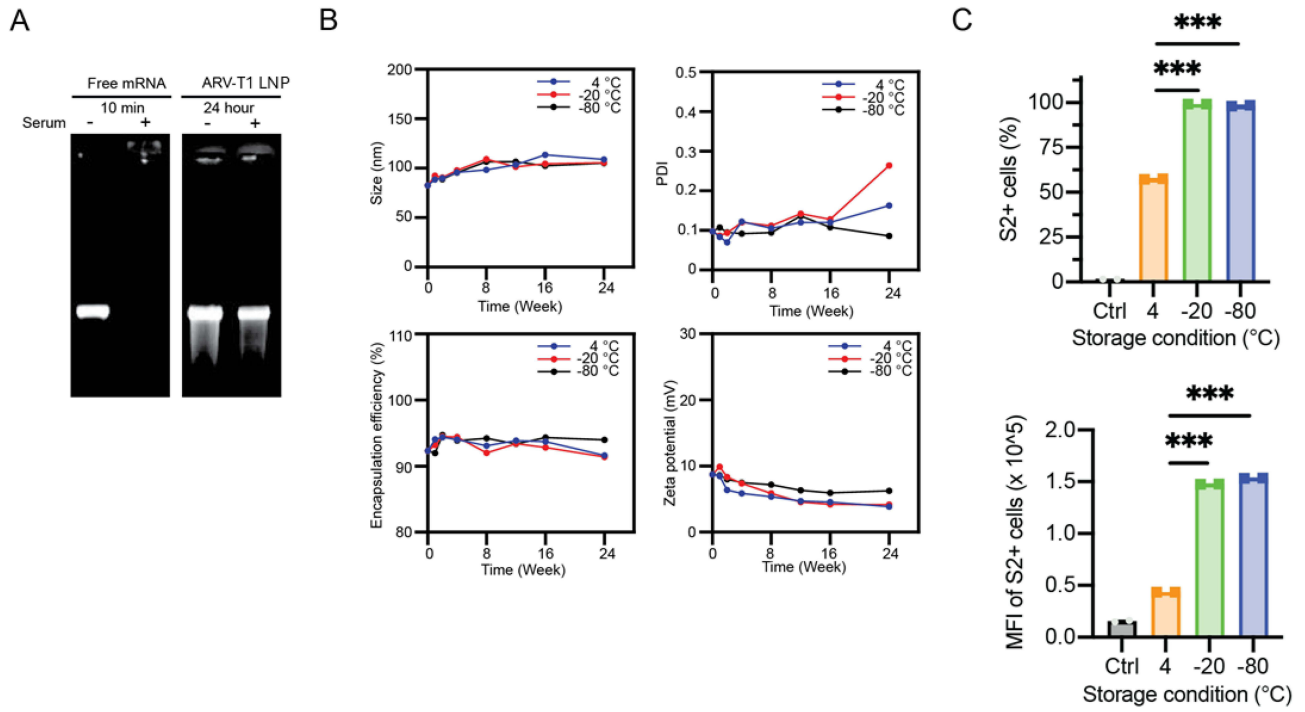

Figure 4 Stability characterization of LNPs formulated with ARV-T1. (**A**) LNPs formulated with ARV-T1 protected the encapsulated SARS-CoV-2 spike protein mRNA from degradation by the enzymes in FBS. (**B**–**C**). Compared to the storage at −80°C, the LNPs formulated with ARV-T1 stored at −20°C for 12 weeks showed no significant difference in particle size, PDI, zeta potential, encapsulation efficacy, and demonstrated similar level of protein expression. Though the PDI increased, and the zeta potential and encapsulation efficacy decreased after 24 weeks of storage of the LNPs formulated with ARV-T1 at −20°C in comparison to storage at −80°C (***$p < 0.005$ compared to the LNPs stored at 4°C).

in the complete degradation of the mRNA, whereas incubation of ARV-T1 formulated LNPs encapsulating SARS-CoV-2 spike protein mRNA for 24 h did not result in degradation of the mRNA. LNPs are susceptible to various physical and chemical changes over time, and their stability during storage is critical for therapeutic efficacy and safety.[18–20] To evaluate the stability of the LNPs formulated with ARV-T1, the LNPs encapsulating SARS-CoV-2 spike protein mRNA were stored either in a deep freezer (−80°C), freezer (−20°C), or refrigerator (4°C) for up to 24 weeks, followed by the analysis of particle size, PDI, zeta potential, encapsulation efficacy, and SARS-CoV-2 spike protein expression. The storage of LNPs formulated with ARV-T1 at −80°C, −20°C, or 4°C did not have a significant effect on particle size or encapsulation efficacy, but the LNPs stored at −20°C or 4°C showed increased PDI compared to those stored at −80°C, especially those LNPs stored at −20°C (Figure 4B). Zeta potential decreased under all three storage conditions (Figure 4B).

The LNPs formulated with ARV-T1 encapsulating SARS-CoV-2 delta variant spike protein mRNA stored at −20°C for 12 weeks showed similar levels SARS-CoV-2 spike protein expression compared to that stored at −80°C after transfection of HEK 293T cells, although the PDI increased after storage at −20°C (Figure 4C). The LNPs stored at 4°C showed ~50% fewer SARS-CoV-2 spike protein positive cells and ~66% lower median fluorescence intensity (MFI) than that of the LNPs stored −20°C and −80°C for 12 weeks (Figure 4C). These results indicate that the storage temperature of LNPs can influence their cellular uptake efficiency, as reflected by the percentage of positive cells and MFI.

Addressing the stability challenges of LNPs is crucial for the development of LNP-based formulations with optimal therapeutic performance and a prolonged shelf life. Pfizer's COVID-19 mRNA vaccine is recommended to be stored at −90 to −60°C, and Moderna's COVID-19 mRNA vaccine is recommended to be stored at −25 to −15°C.[21,22] Our data demonstrated that LNPs formulated with ARVT1 encapsulating SARS-CoV-2 spike protein mRNA stored −20°C showed similar levels of protein expression compared to those stored at −80°C, indicating LNPs formulated with ARV-T1 are comparable to Moderna's COVID-19 mRNA vaccine and more stable than Pfizer's COVID-19 mRNA vaccine. Although

the storage of ARV-T1 formulated LNPs at −20°C for 24 weeks slightly increased PDI, it did not have any effect on the delivery of mRNA or the expression of recombinant proteins.

The mRNA-LNPs Formulated with ARV-T1 Showed Longer Period of Protein Expression with Increased Level After IM Injection in Mice as Compared to That of mRNA-LNPs Formulated with SM-102

To evaluate the in vivo delivery efficacy of LNPs formulated with novel ionizable lipid ARV-T1, time-dependent organ luminescence was quantified after IM injection into the flanks of BALB/c mice (n = 6) at a dose of 1μg Luc mRNA encapsulated in LNPs formulated with ARV-T1 and SM-102 as a control. Luciferase expression was highest at 6 h post-injection for the LNPs formulated with SM-102, but the signal quickly faded, and luminescence was barely detectable 72 h after injection (Figure 5A). In contrast, the mice injected with LNPs formulated with ARV-T1 showed strong luminance signal 6 h after injection, reached peak levels at 24 h, slightly decreased at 48 h, and 50% signal of peak level still remained 72 h post-injection (Figure 5A).

The peak level of luminescence from LNPs formulated with ARV-T1 was comparable to that of LNPs formulated with SM-102, but lasted much longer. These data indicated that the mRNA delivered with the LNPs formulated with ARV-T1 had stronger protein expression and longer protein expression in vivo (Figure 5A and B). The LNPs formulated with ARV-T1 demonstrated superior performance in vivo, possibly because of their smaller sizes and higher level of mRNA escape, which resulted in slower clearance by the immune system and longer periods of protein expression.[8,23]

SARS-CoV-2 Spike Protein mRNA Formulated with ARV-T1 Elicited Markedly Higher Binding Antibodies and Virus Neutralizing Antibodies as Compared to That of LNPs Formulated with SM-102

BALB/c mice were immunized twice, 3 weeks apart, with LNPs encapsulating SARS-CoV-2 delta variant spike protein mRNA formulated with ARV-T1 in comparison to SM-102, and PBS as a negative control. Humoral responses to spike

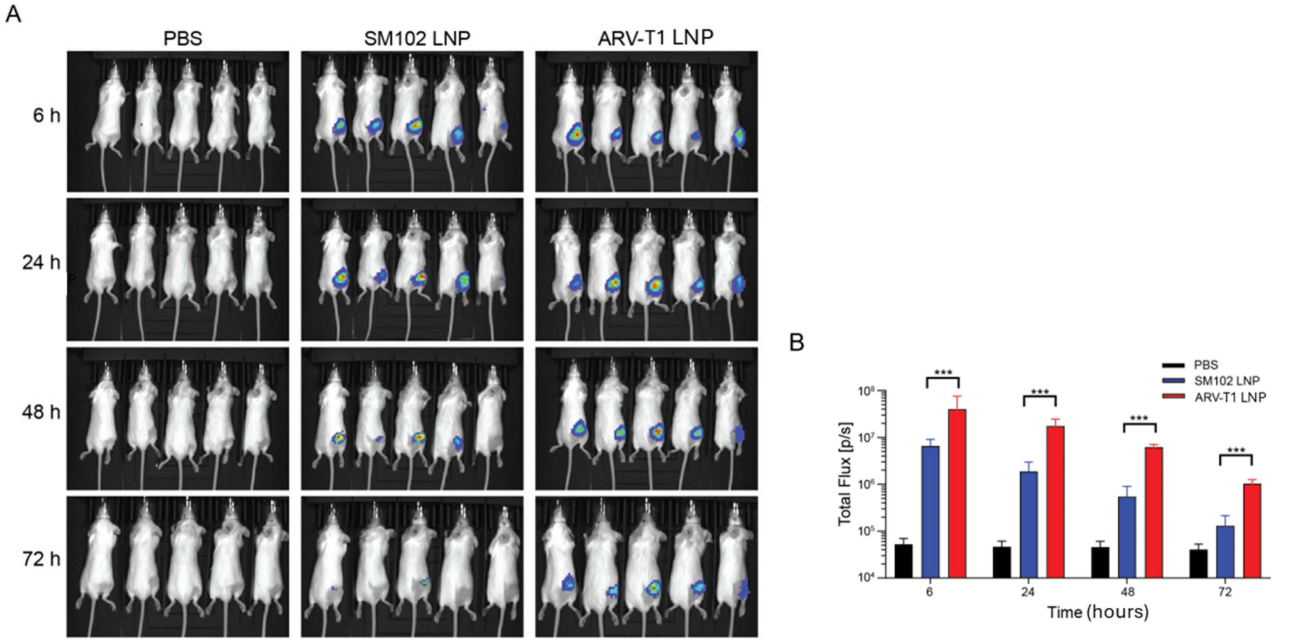

Figure 5 In vivo delivery of mRNA and protein expression by LNPs formulated with ARV-T1 were significantly higher than that of SM-102. In vivo imaging studies showed superior mRNA delivery by LNPs formulated with ARV-T1 compared to SM-102. (**A**) BALB/c mice were injected LNPs formulated with ARV-T1 versus SM-102 encapsulating firefly luciferase mRNA, luminance was captured by in vivo imaging 6, 24, 48 and 72 hours after injection. (**B**) Luciferase signal was plotted in bar graphs. LNPs formulated with ARV-T1 showed longer period of protein expression with increased level after IM injection in mice as compared to that of mRNA-LNPs formulated with SM-102 (***$p < 0.005$ compared to the mice injected with LNPs formulated with SM-102).

https://doi.org/10.2147/IJN.S527822

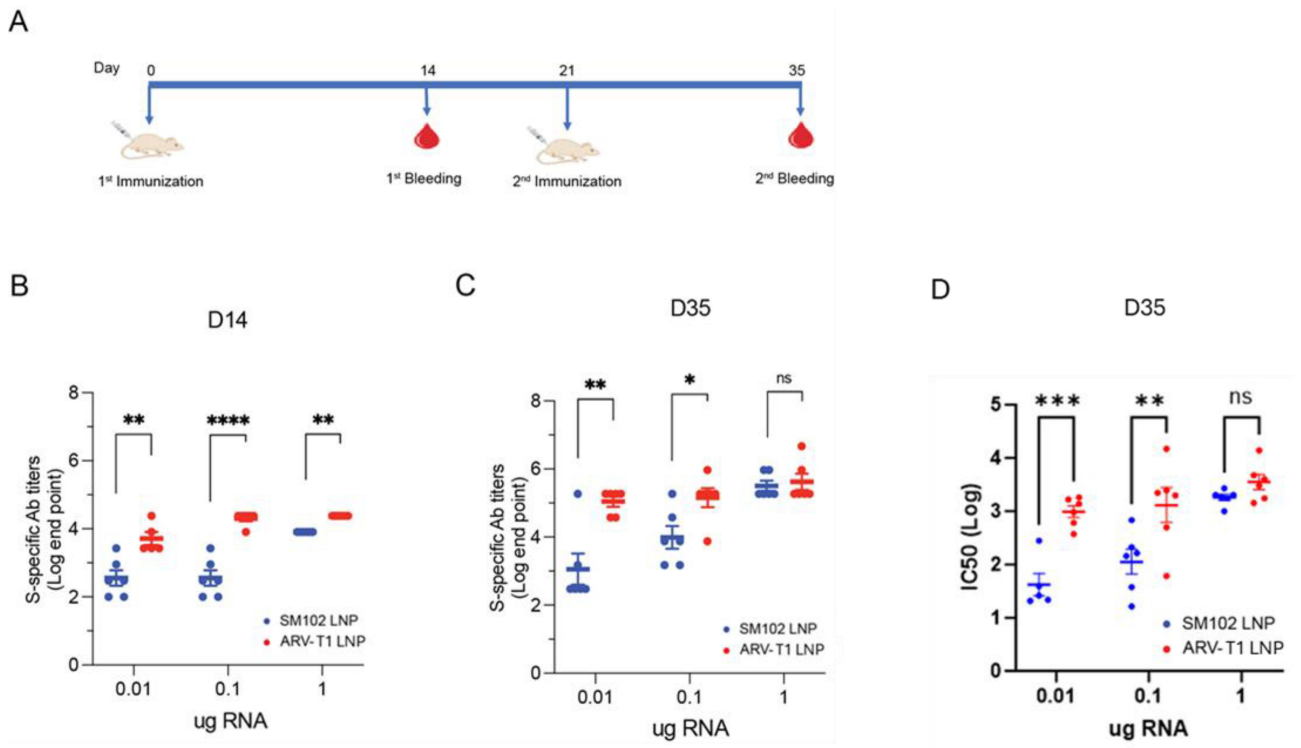

Figure 6 LNPs formulated with ARV-T1 encapsulating SARS-CoV-2 spike protein mRNA elicited markedly higher binding antibodies and virus neutralizing antibodies as compared to that of LNPs formulated with SM-102. (**A**) Diagram of mouse immunization. BALB/c mice were immunized twice with LNPs encapsulating SARS-CoV-2 spike protein mRNA formulated with ARV-T1 in comparison to SM-102 3 weeks apart. (**B** and **C**) SARS-CoV-2 spike protein binding antibodies titers 14 and 35 days after the first immunization. (**D**) SARS-CoV-2 virus neutralizing antibodies 35 days after the first immunization analyzed using pseudo typed virus (*, **, ***, and ****indicate $p < 0.05$, 0.01, 0.005 and 0.001 respectively as compared to mice immunized with the LNPs formulated with SM-102).

protein were analyzed two weeks after the second immunization (Figure 6A). Low dose (0.01 and 0.1 μg) LNPs formulated with ARV-T1 induced more than 10-fold higher binding antibodies (IgG) to the SARS-CoV-2 spike protein than the LNPs formulated with SM-102, whereas high-dose (1 μg) LNPs formulated with ARV-T1 induced comparable spike protein binding antibodies to that of LNPs formulated with SM-102 (Figure 6B and C). This suggests that the high-dose (1 μg) LNPs formulated with either ARV-T1 or SM-102 elicited maximum spike protein binding antibodies, and the antibody response was saturated. As 0.1 μg LNPs formulated with ARV-T1 induced similar level spike protein binding antibodies to that of 1 μg LNPs formulated with SM-102, it is suggested that LNPs formulated with ARV-T1 is 10-fold more potent than LNPs formulated with SM-102 in inducing binding antibodies.

The neutralizing antibody was analyzed using a SARS-CoV-2 pseudotyped virus, and the half maximal inhibitory concentration (IC50) geometric mean titer (GMT) was determined. Similar to the SARS-CoV-2 spike protein binding antibodies, mice immunized with low dose (0.01 and 0.1 μg) LNPs formulated with ARV-T1 induced more than 10-fold higher virus neutralizing antibodies compared to that of the LNPs formulated with SM-102, whereas high dose LNPs formulated with ARV-T1 induced neutralizing antibodies comparable to that of LNPs formulated with SM-102 (Figure 6D). More importantly, the 0.1 μg LNPs formulated with ARV-T1 elicited SARS-CoV-2 neutralizing antibodies equivalent to that of 1 μg LNPs formulated with either ARV-T1 or SM-102, indicating that low-dose LNPs formulated with ARV-T1 could induce an optimal immune response (Figure 6D). Lower doses usually result in fewer adverse effects. Since 0.1 μg LNPs formulated with ARV-T1 induced comparable levels of SARS-CoV-2 virus neutralizing antibodies to that of 1 μg LNP formulated with SM-102, it indicates that LNPs formulated with ARV-T1 is 10-fold more potent than the LNPs formulated with SM-102 in inducing virus neutralizing antibodies. The advantage of LNPs formulated with ARV-T1 over that of SM-102 was likely due to their smaller sizes, higher rate of mRNA escape, higher antigen protein expression that lasted for a longer period of time.

LNPs Formulated with ARV-T1 Encapsulating SARS-CoV-2 Spike Protein mRNA Showed Minimal Toxicity in vitro and in vivo

To assess the potential cytotoxicity of mRNA-LNPs in vitro, Huh7 (suspension) and HEK 293T (adherent) cell lines were incubated with different concentrations of LNPs formulated with ARV-T1 versus SM-102 encapsulating the SARS-CoV-2 delta variant spike protein mRNA in 24 well-plates for 48 h. Cell viability was studied using an XTT assay 48 h after the addition of the LNPs. There was no significant change in the viability of either cell line (Huh7 and HEK 293T) after 48 h of incubation with LNPs formulated with either ARV-T1 or SM-102, except at very high concentration (125 µM) in Huh-7 cells (Figure 7A).

To study the potential in vivo toxicity of ARV-T1, BALB/c mice were injected twice at 3-week intervals with LNPs formulated with ARV-T1 versus SM-102 encapsulating the SARS-CoV-2 delta variant spike protein mRNA (Figure 7B). One day after the last immunization, a blood biochemistry test revealed no abnormal findings (Figure 7C). Two weeks after the last immunization, immunohistochemical analysis of the liver, heart, and kidney did not reveal any abnormal changes (Figure 7C and E). Furthermore, the body weights of the mice did not change significantly (Figure 7D).

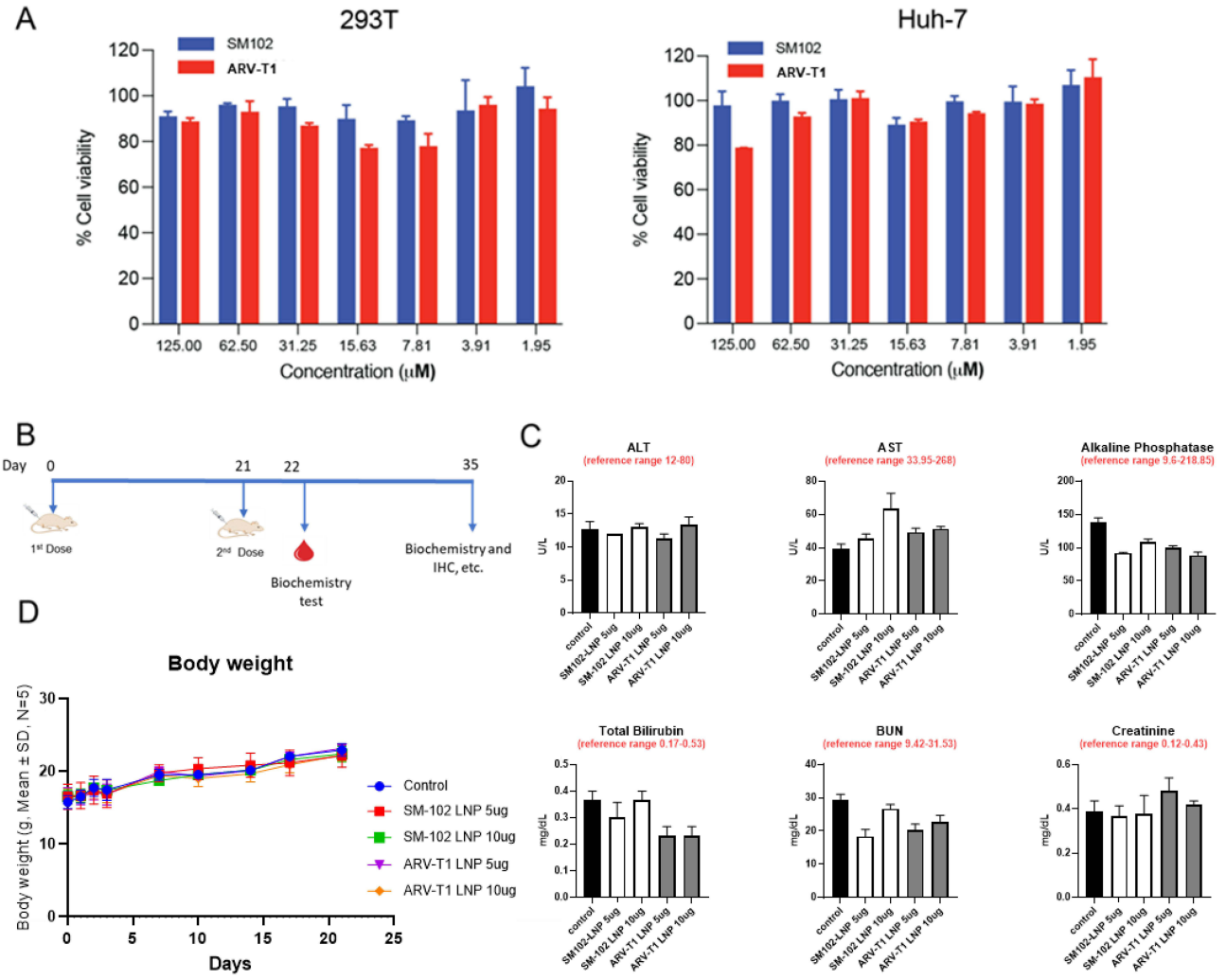

Figure 7 LNPs formulated with ARV-T1 had excellent toxicity profile, and showed minimal toxicity both in vitro and in vivo. (**A**) In vitro toxicity study with HEK293 and Huh-7 cell lines, a range of 64-fold gradually increased concentrations of LNPs formulated with ARV-T1 encapsulating SARS-CoV-2 spike protein mRNA did not induce cytotoxicity, and showed no difference as compared to the LNPs formulated with SM-102. (**B**–**D**) Mouse in vivo toxicity study. BALB/c mice were injected twice at 3 week intervals with LNPs formulated with ARV-T1 versus SM-102 encapsulating SARS-CoV-2 spike protein, biochemistry analysis of liver and kidney functions 1 day post the last injection, and immunohistochemical analysis of the liver 14 days post the last injection did not show abnormal changes.

https://doi.org/10.2147/IJN.S527822

Discussion

The delivery of RNAs to target cells by LNPs provides vast opportunities to tackle a series of life- threatening diseases, including gene editing, RNA interface therapies, and vaccines, particularly mRNA vaccines against infectious diseases and cancers.[1,3,5] LNPs typically consist of four components: ionizable lipids, phospholipids, cholesterol, and PEGylated lipids, where the ionizable lipid plays the critical role in RNA encapsulation, LNP endocytosis, RNA endosomal escape as well as eliciting potent immune responses.[7,8,24] Ionizable lipids are positively charged at acidic pH during LNP manufacturing to condense negatively charged RNAs through electrostatic interactions that enable efficient encapsulation of RNAs in LNPs, typically >90%.[8,25] It is reported that at physiological pH 7.4, according to the Henderson–Hasselbalch equation, approximately 10% of the ionizable lipids in LNPs with an apparent pKa of ~6.4 are positively charged, which could facilitate endocytosis of LNPs through the surface charge or the proteins bond on the surface of LNPs.[8,26] Endosomal escape of the mRNA encapsulated in LNPs is the most critical step in LNP vaccination and therapy, as studies showed that less than 5% of RNAs loaded into LNPs escape from the endosomes into the cytosol.[27,28] Endosomal escape is mediated by the fusion of LNP with the endosomal membrane in an acidic environment, which leads to disruption of the endosomal membrane and results in the release of RNAs encapsulated in LNPs into the cytosol.[1,7] LNPs induce pro-inflammatory cytokine production and thus have an adjuvant effect in mRNA vaccines, and therefore help with the development of robust immune responses.[29,30] It has been reported that ionizable lipids with apparent pKa between 6.6 and 6.9 are optimal for immunogenicity, and the size, shape, and rigidity of LNPs are important factors in immunological activation.[8,14,24]

Although ionizable lipids with diverse chemical identities have been created since 2008, the development of novel ionizable lipids holds great promise in improving the efficacy and safety of LNPs.[1,7,8] Upon chemical modification of the butanolamine head group with cholesterol and alkoxy alkanoate moieties, a novel ionizable lipid, ARV-T1, was synthesized. Compared to SM-102, the ionizable lipid used in the Moderna SARS-CoV-2 vaccine, the LNPs formulated with ARV-T1 showed smaller particle size, lower polydispersity index, and higher absolute zeta potential value. ARV-T1 has a pKa value of 6.73, which is close to the pKa of SM-102 (6.53) and the pKa values of other commercially available ionizable lipids ALC-0315 (6.38), C12-200 (6.81), and DLin-MC3-DMA (6.53). The pKa of the ionizable lipid ARV-T1 makes it optimal for both the encapsulation of mRNA and induction of the immune response.[8,14,24] The LNPs formulated with ARV-T1 had about 80 nm mean hydrodynamic size, which was smaller than the 90 nm size of the LNPs formulated with SM-102. It has been reported that the particle size of LNP has a significant effect on the immunogenicity of mRNA-LNPs, with 50 nm size LNP inducing an optimal immune response; therefore, the smaller size LNPs formulated with ARV-T1 could contribute to higher immunogenicity compared to the LNPs formulated with SM-102[3]. The absolute zeta potential value (10 mV) of the LNPs formulated with ARV-T1 was higher than that of the LNPs formulated with SM102 (5 mV), indicating higher nucleic acid encapsulation efficacy of ARV-T1, as higher charge of ionizable lipid is associated with more efficient encapsulation of nucleic acid in LNPs formulated.[8,16] This was demonstrated in our experiment that the encapsulation efficacy of the LNPs formulated with ARV-T1 was slightly higher than that of SM-102, and the LNPs formulated with both ARV-T1 and SM-102 had RNA encapsulation efficacy above 90%.

Addressing the stability challenges of LNP is crucial for the development of LNP-based formulations with prolonged shelf life and optimal therapeutic performance. The factors contributing to LNP stability are temperature, humidity, pH, light exposure, protein interactions, and ionic interactions, and consequences of instability could result in changes in LNP size that could affect their biodistribution, cellular uptake, and clearance kinetics.[18,20,31] Encapsulation efficiency decrease due to instability could cause loss of encapsulated cargo that reduce the therapeutic payload delivered to target cells. LNPs formulated with ARV-T1 stored at −20°C for 12 weeks showed no significant differences in particle size, PDI, zeta potential, encapsulation efficacy, and demonstrated similar levels of protein expression as compared to the LNPs stored at −80°C. These results indicate that LNPs formulated with ARV-T1 are comparable to Moderna's COVID-19 mRNA vaccine and more stable than Pfizer's COVID-19 mRNA vaccine, which are recommended to be stored at −25 to −15°C and −90 to −60°C respectively.[21,22] Although the storage of LNPs formulated with ARV-T1 at −20°C for extended period (24 weeks) had slightly increased PDI, it did not have any effect on the delivery of mRNA.

After LNPs are endocytosed by target cells, endosomal escape plays a critical role in the delivery of RNAs encapsulated in the LNPs.[1,3] As endosomes mature, the pH inside the endosomes decreases to below the apparent pKa of the ionizable lipids, and the ionizable lipids are protonated and become positively charged.[1,7] The electrostatic interactions between the cationic ionizable lipids in the LNPs and the anionic endosomal phospholipids lead to the transition of the planar bilayer structure within the endosomal membrane to an inverted hexagonal H_{II} phase, which facilitates membrane fusion and disruption, resulting in endosomal escape and cargo release into the cytosol.[1,8,9] The tail of ionizable lipids plays a more important role in the formation of an inverted cone-shaped structure and RNA escape, as multi-tail ionizable lipids and branched-tail ionizable lipids produce a more cone-shaped structure with enhanced endosome-disrupting ability due to the increased cross-section of the tail region, resulting in increased endosomal escape of RNA.[7,32,33] ARV-T1 has three tails, where one tail with a cholesterol moiety incorporated, which significantly increases the cross section of its tail region compared to SM-102 that also has three tails, and could lead to significantly increased endosomal escape. As a result, the SARS-CoV-2 mRNA formulated with ARV-T1 demonstrated a 7-fold increase in spike protein expression in vitro compared to the SARS-CoV2 mRNA formulated with SM-102.

Achieving decent transfection efficiency and response in a dose-dependent manner are key indicators of the effectiveness of a delivery system for genetic material.[1,8,34] The ability of LNPs formulated with ARV-T1 to effectively deliver plasmid DNA suggests its potential application in various gene therapy strategies, where the introduction of specific genes into target cells is desired. This could include gene editing, gene silencing, or the delivery of therapeutic genes for treating genetic disorders, cancers, or other diseases.[34–36]

The LNPs formulated with ARV-T1 not only demonstrated superior performance in vitro but also showed a longer period of protein expression with increased levels after IM injection in mice compared to that of mRNA-LNPs formulated with SM-102. These were possibly due to the smaller size of LNPs formulated with ARV-T1 and their higher-level mRNA escape, which resulted in slower clearance by the immune system, longer period and high level protein expression.[8,23] The cholesterol moiety incorporated in the tail of ARV-T1 could increase the rigidity of the formulated LNPs, which would also increase the retention of the LNPs in tissues and could further increase protein expression.[37]

The advantages of LNPs formulated with ARV-T1 over that SM-102 are their smaller sizes, higher rate of mRNA escape, and higher antigen protein expression that lasts longer period of time. As a result, the SARS-CoV-2 spike protein mRNA formulated with ARV-T1 elicited more than 10-fold higher titers of binding antibodies and virus neutralizing antibodies as compared to that of LNPs formulated with SM-102. The results suggest that LNPs formulated with ARV-T1 encapsulating SARS-CoV-2 spike protein mRNA could serve as a better vaccine candidate against SARS-CoV-2 than currently approved vaccines, such as Spikevax®. These findings underscore the importance of lipid nanoparticle formulations in modulating the immunogenicity of mRNA vaccines. LNPs formulated with ARV-T1 may offer a promising platform for enhancing vaccine efficacy by improving protein expression and immune responses to generate vaccines against various viruses and cancers.

The ionizable lipid ARV-T1 contains a tertiary amine with ester-containing lipid tails and these structural features enable rapid in vivo metabolism, as demonstrated in our study, the LNPs formulated with ARV-T1 encapsulating SARS-CoV-2 spike protein mRNA showed minimal toxicity in vitro and in vivo. These features could improve the biocompatibility and clearance of LNPs formulated with ARV-T1 and pave the way for their clinical use.[1,7,8]

Conclusion

The novel proprietary ionizable lipid ARV-T1 holds great promise as a key component in mRNA LNP formulations. The key advantages of LNPs formulated with ARV-T1 over existing ionizable lipids such as SM-102 are their smaller particle sizes, lower polydispersity indices, and higher absolute zeta potential values. ARV-T1 has a pKa value of 6.73, which makes it optimal for both encapsulation of mRNA and induction of immune response.[8,14,24] The small head group of ARV-T1 allows it to adopt an inverted hexagonal non-bilayer structure, and its asymmetric tail incorporating a cholesterol moiety contributes to increased endosomal membrane fusion-mediated delivery of mRNA cargo to the cytosol of target cells by escaping endosomal degradation upon acidification.[14,15] LNPs formulated with ARV-T1 showed increased mRNA delivery both in vitro and in vivo, demonstrated increased levels of protein expression that lasted for

a significantly longer period, and induced markedly higher titers of binding antibodies and virus neutralizing antibodies compared to existing ionizable lipids in clinical use. Furthermore, the unique ester linkage of ARV-T1 enables facile metabolism, with improved biocompatibility and safety profiles. The results indicated that LNPs formulated with the novel ionizable lipid ARV-T1 could be a promising platform for the development of RNA/DNA-based therapies, such as highly efficient vaccines for viruses and cancers.

Disclosure

Ju Hyeong Jeon, Huabin Zhu, Jane Qin, Laura Katherine Langston, Renhuan Xu and Xinle Cui are currently employed by ARV Technologies, Stephanie Mou and Ramesh Marasini are former employees. Huabin Zhu reports a patent Sterol Based Ionizable Lipids and Lipid Nanoparticles pending to PCT/US23/29742. Jianzhu Chen, Luyao Wang, and Shuna Li collaborated with this study. ARV Technologies filed patents for ARV-T1. Jianzhu Chen reports personal fees from ARV Technologies, Inc., during the conduct of the study; personal fees from ARV Technologies, Inc., outside the submitted work; and Jianzhu Chen is a co-founder of ARV Technologies, Inc. and serves on its Scientific Advisory Board. The authors report no other conflicts of interest in this work.

References

1. Hou X, Zaks T, Langer R, Dong Y. Lipid nanoparticles for mRNA delivery. *Nat Rev Mater*. 2021;6(12):1078–1094. doi:10.1038/s41578-021-00358-0
2. Kulkarni JA, Witzigmann D, Thomson SB, et al. The current landscape of nucleic acid therapeutics. *Nat Nanotechnol*. 2021;16(6):630–643. doi:10.1038/s41565-021-00898-0
3. Gote V, Bolla PK, Kommineni N, et al. A comprehensive review of mRNA vaccines. *Int J Mol Sci*. 2023;24(3):2700. doi:10.3390/ijms24032700
4. Al Fayez N, Nassar MS, Alshehri AA, et al. Recent advancement in mRNA vaccine development and applications. *Pharmaceutics*. 2023;15(7):1972. doi:10.3390/pharmaceutics15071972
5. Swetha K, Kotla NG, Tunki L, et al. Recent advances in the lipid nanoparticle-mediated delivery of mRNA vaccines. *Vaccines*. 2023;11(3). doi:10.3390/vaccines11030658
6. Tenchov R, Bird R, Curtze AE, Zhou Q. Lipid nanoparticles horizontal line from liposomes to mRNA vaccine delivery, a landscape of research diversity and advancement. *ACS Nano*. 2021;15(11):16982–17015. doi:10.1021/acsnano.1c04996
7. Han X, Zhang H, Butowska K, et al. An ionizable lipid toolbox for RNA delivery. *Nat Commun*. 2021;12(1):7233. doi:10.1038/s41467-021-27493-0
8. Hald Albertsen C, Kulkarni JA, Witzigmann D, Lind M, Petersson K, Simonsen JB. The role of lipid components in lipid nanoparticles for vaccines and gene therapy. *Adv Drug Deliv Rev*. 2022;188:114416. doi:10.1016/j.addr.2022.114416
9. Schlich M, Palomba R, Costabile G, et al. Cytosolic delivery of nucleic acids: the case of ionizable lipid nanoparticles. *Bioeng Transl Med*. 2021;6(2):e10213. doi:10.1002/btm2.10213
10. Nelson J, Sorensen EW, Mintri S, et al. Impact of mRNA chemistry and manufacturing process on innate immune activation. *Sci Adv*. 2020;6(26):eaaz6893. doi:10.1126/sciadv.aaz6893
11. Fukami T, Yokoi T. The emerging role of human esterases. *Drug Metab Pharmacokinet*. 2012;27(5):466–477. doi:10.2133/dmpk.dmpk-12-rv-042
12. Sabnis S, Kumarasinghe ES, Salerno T, et al. A novel amino lipid series for mRNA delivery: improved endosomal escape and sustained pharmacology and safety in non-human primates. *Mol Ther*. 2018;26(6):1509–1519. doi:10.1016/j.ymthe.2018.03.010
13. Hassett KJ, Benenato KE, Jacquinet E, et al. Optimization of lipid nanoparticles for intramuscular administration of mRNA vaccines. *Mol Ther Nucleic Acids*. 2019;15:1–11. doi:10.1016/j.omtn.2019.01.013
14. Jayaraman M, Ansell SM, Mui BL, et al. Maximizing the potency of siRNA lipid nanoparticles for hepatic gene silencing in vivo. *Angew Chem Int Ed Engl*. 2012;51(34):8529–8533. doi:10.1002/anie.201203263
15. Chatterjee S, Kon E, Sharma P, Peer D. Endosomal escape: a bottleneck for LNP-mediated therapeutics. *Proc Natl Acad Sci U S A*. 2024;121(11):e2307800120. doi:10.1073/pnas.2307800120
16. Jung HN, Lee SY, Lee S, Youn H, Im HJ. Lipid nanoparticles for delivery of RNA therapeutics: current status and the role of in vivo imaging. *Theranostics*. 2022;12(17):7509–7531. doi:10.7150/thno.77259
17. Marasini R, Rayamajhi S, Moreno-Sanchez A, Aryal S. Iron(iii) chelated paramagnetic polymeric nanoparticle formulation as a next-generation T(1)-weighted MRI contrast agent. *RSC Adv*. 2021;11(51):32216–32226. doi:10.1039/d1ra05544e
18. Oude Blenke E, Ornskov E, Schoneich C, et al. The storage and in-use stability of mRNA vaccines and therapeutics: not A cold case. *J Pharm Sci*. 2023;112(2):386–403. doi:10.1016/j.xphs.2022.11.001
19. Kim B, Hosn RR, Remba T, et al. Optimization of storage conditions for lipid nanoparticle formulated self-replicating RNA vaccines. *J Control Release*. 2023;353:241–253. doi:10.1016/j.jconrel.2022.11.022
20. Young RE, Hofbauer SI, Riley RS. Overcoming the challenge of long-term storage of mRNA-lipid nanoparticle vaccines. *Mol Ther*. 2022;30(5):1792–1793. doi:10.1016/j.ymthe.2022.04.004
21. Schoenmaker L, Witzigmann D, Kulkarni JA, et al. mRNA-lipid nanoparticle COVID-19 vaccines: structure and stability. *Int J Pharm*. 2021;601:120586. doi:10.1016/j.ijpharm.2021.120586
22. Hermosilla J, Alonso-Garcia A, Salmeron-Garcia A, et al. Analysing the in-use stability of mRNA-LNP COVID-19 vaccines comirnaty (Pfizer) and spikevax (Moderna): a comparative study of the particulate. *Vaccines*. 2023;11(11):1635. doi:10.3390/vaccines11111635
23. Li SD, Huang L. Pharmacokinetics and biodistribution of nanoparticles. *Mol Pharm*. 2008;5(4):496–504. doi:10.1021/mp800049w
24. Heuts J, Jiskoot W, Ossendorp F, van der Maaden K. Cationic nanoparticle-based cancer vaccines. *Pharmaceutics*. 2021;13(5):596. doi:10.3390/pharmaceutics13050596

25. Leung AK, Tam YY, Chen S, Hafez IM, Cullis PR. Microfluidic mixing: a general method for encapsulating macromolecules in lipid nanoparticle systems. *J Phys Chem B*. 2015;119(28):8698–8706. doi:10.1021/acs.jpcb.5b02891
26. Francia V, Schiffelers RM, Cullis PR, Witzigmann D. The biomolecular corona of lipid nanoparticles for gene therapy. *Bioconjug Chem*. 2020;31(9):2046–2059. doi:10.1021/acs.bioconjchem.0c00366
27. Sahay G, Querbes W, Alabi C, et al. Efficiency of siRNA delivery by lipid nanoparticles is limited by endocytic recycling. *Nat Biotechnol*. 2013;31(7):653–658. doi:10.1038/nbt.2614
28. Gilleron J, Querbes W, Zeigerer A, et al. Image-based analysis of lipid nanoparticle-mediated siRNA delivery, intracellular trafficking and endosomal escape. *Nat Biotechnol*. 2013;31(7):638–646. doi:10.1038/nbt.2612
29. Alameh MG, Tombacz I, Bettini E, et al. Lipid nanoparticles enhance the efficacy of mRNA and protein subunit vaccines by inducing robust T follicular helper cell and humoral responses. *Immunity*. 2021;54(12):2877–2892e7. doi:10.1016/j.immuni.2021.11.001
30. Pizzuto M, Gangloff M, Scherman D, et al. Toll-like receptor 2 promiscuity is responsible for the immunostimulatory activity of nucleic acid nanocarriers. *J Control Release*. 2017;247:182–193. doi:10.1016/j.jconrel.2016.12.029
31. Ball RL, Bajaj P, Whitehead KA. Achieving long-term stability of lipid nanoparticles: examining the effect of pH, temperature, and lyophilization. *Int J Nanomed*. 2017;12:305–315. doi:10.2147/IJN.S123062
32. Akinc A, Zumbuehl A, Goldberg M, et al. A combinatorial library of lipid-like materials for delivery of RNAi therapeutics. *Nat Biotechnol*. 2008;26(5):561–569. doi:10.1038/nbt1402
33. Hajj KA, Ball RL, Deluty SB, et al. Branched-tail lipid nanoparticles potently deliver mRNA in vivo due to enhanced ionization at endosomal pH. *Small*. 2019;15(6):e1805097. doi:10.1002/smll.201805097
34. Cullis PR, Hope MJ. Lipid nanoparticle systems for enabling gene therapies. *Mol Ther*. 2017;25(7):1467–1475. doi:10.1016/j.ymthe.2017.03.013
35. Zong Y, Lin Y, Wei T, Cheng Q. Lipid nanoparticle (LNP) enables mRNA delivery for cancer therapy. *Adv Mater*. 2023;35(51):e2303261. doi:10.1002/adma.202303261
36. Kiaie SH, Majidi Zolbanin N, Ahmadi A, et al. Recent advances in mRNA-LNP therapeutics: immunological and pharmacological aspects. *J Nanobiotechnology*. 2022;20(1):276. doi:10.1186/s12951-022-01478-7
37. Benne N, van Duijn J, Kuiper J, Jiskoot W, Slutter B. Orchestrating immune responses: how size, shape and rigidity affect the immunogenicity of particulate vaccines. *J Control Release*. 2016;234:124–134. doi:10.1016/j.jconrel.2016.05.033